J. Plasma Physics (2002), *vol.* 67, *parts* 2&3, *pp.* 115–127.
DOI: 10.1017/S0022377801001593 Printed in the United Kingdom

Nonlinear electrostatic oscillations in a dusty plasma

H. HOUILI, M. TRIBÈCHE and T. H. ZERGUINI

Theoretical Physics Laboratory, The Physics Institute, USTHB, BP 32 El Alia, Algiers 16111, Algeria

(Received 8 January 2001)

Abstract. Stationary nonlinear one-dimensional electrostatic oscillations in a plasma containing dust grains with variable charge are considered through a cold-beam model. The new constraints brought by the presence of dusts on the BGK modes are clarified and the appearance of a soliton mode that was not present in the fixed-charge problem is investigated.

1. Introduction

Dusty-plasma phenomena have attracted a good deal of interest during the last ten years or so because of their wide relevance in both laboratory and space contexts. The charge carried by the dust grains and its variation in space and time can to some degree or another affect plasma waves (Ma and Yu 1994; Vladimirov et al. 1998). Recently, the influence of dust on nonlinear plasma electrostatic oscillations has been investigated (Tribèche et al. 2000) through a cold kinetic model, but the dynamics of charging was not considered. We propose here to generalize this analysis to the case of variable-charge grains.

2. Basic equations

Stationary nonlinear electrostatic waves in a collisionless plasma in one space dimension are governed by the Vlasov–Poisson equation (Bernstein et al. 1957)

$$v\frac{\partial f_j(x,v)}{\partial x} + \frac{q_j}{m_j}\frac{\partial \phi(x)}{\partial x}\frac{\partial f_j(x,v)}{\partial v} = 0, \tag{1}$$

$$\frac{\partial^2 \phi(x)}{\partial x^2} = -4\pi \sum_{j=e,i,d} q_j \int f_j(x,v)\, dv, \tag{2}$$

where $j = e, i$ and d for electrons, ions and dust grains respectively. The general solution of (1) may be written as

$$f_j = f_j(E_j), \tag{3}$$

where the energy E_j for electrons and ions is given by

$$E_{e,i} = \tfrac{1}{2} m_{e,i} v^2 \mp e\phi, \tag{4}$$

whereas for grains of variable charge it becomes

$$E_d = \tfrac{1}{2} m_d v^2 + \int_0^\phi q_d \, d\phi. \tag{5}$$

Following Tribèche et al. (2000), we consider cold beams for electrons, ions and dust grains:

$$f_j(v) = n_{j0} \frac{v_{j0}}{\tilde{v}_j} \delta(v - \tilde{v}_j), \tag{6}$$

with

$$\tilde{v}_{e,j} = v_{e,i0} \sqrt{1 \pm \frac{2e}{m_{e,i} v_{e,i}^2} \phi}, \tag{7}$$

$$\tilde{v}_d = v_{d0} \sqrt{1 + \frac{2e}{m_d v_{d0}^2} \int_0^\phi Z \, d\phi}. \tag{8}$$

Here Z is the grain charge number and v_{j0} are arbitrary constants large enough so that (7) and (8) yield real positive values for $\tilde{v}_j$. We introduce the dimensionless variables

$$\psi = \frac{2e}{W_j} \phi, \qquad X = \frac{\omega_j}{v_{j0} x}$$

where $W_j = m_j v_{j0}^2$ and ω_j is the j-species plasma frequency. Thus the Poisson equation (2) for untrapped particles is

$$\frac{d^2\psi}{dX^2} = \frac{2}{f\sqrt{1+\alpha\psi}} - \frac{2}{\sqrt{1-\psi}} + \frac{2\varepsilon Z}{\sqrt{1+\chi/\beta}}, \tag{9}$$

with χ the grain's normalized 'potential energy'

$$\chi = \int_0^\psi Z \, d\psi, \tag{10}$$

and

$$\alpha = \frac{W_i}{W_e}, \qquad \beta = \frac{W_d}{W_i}, \qquad \varepsilon = \frac{n_{d0}}{n_{i0}}, \qquad f = \frac{n_{i0}}{n_{e0}}. \tag{11}$$

The dust charge is determined by the charge-conservation equation

$$v_d \frac{dq_d}{dx} = I_e + I_i, \tag{12}$$

where, for our cold model, the electron and ion currents are given by (Barnes et al. 1992):

$$I_e = -\pi r^2 e n_{e0} v_{e0} \left(1 + \frac{2eq_d}{r m_e v_e^2}\right), \tag{13}$$

$$I_i = \pi r^2 e n_{i0} v_{i0} \left(1 - \frac{2eq_d}{r m_i v_i^2}\right), \tag{14}$$

with r being the grain radius.

Thus, in addition to the Poisson equation (9), we obtain the following two equations for 'potential energy' and charge variation:

$$\frac{d\chi}{dX} = Z \frac{d\psi}{dX}, \tag{15}$$

$$\frac{dZ}{dX} = \frac{1}{\sqrt{1+\chi/\beta}}\left[-A\left(1+\frac{BZ}{1-\psi}\right)+C\left(1-\frac{DZ}{1+\alpha\psi}\right)\right], \tag{16}$$

where

$$A = \pi r^2 n_{i0}\frac{v_{i0}^2}{v_{d0}\omega_i}, \qquad B = \frac{2e^2}{rWi}, \tag{17}$$

$$C = \pi r^2 n_{e0}\frac{v_{e0}v_{i0}}{v_{d0}\omega_i}, \qquad D = \frac{2e^2}{rW_e}. \tag{18}$$

Within the characteristic time of the charging process, the dust displacement is negligible, so we set $I_e + I_i = 0$ and obtain

$$Z = Z_0\frac{(1-\psi)(1+\alpha\psi)}{1+p\psi}, \tag{19}$$

where

$$Z_0 = \frac{rW_i}{2e^2}\frac{v_{e0}-fv_{i0}}{\alpha v_{e0}+fv_{i0}}, \tag{20}$$

$$p = -\alpha\frac{v_{e0}-fv_{i0}}{\alpha v_{e0}+fv_{i0}}, \tag{21}$$

and

$$\chi = \frac{Z_0}{p^3}(p^2+p-\alpha p-\alpha)\ln(1+p\psi) - \frac{Z_0\alpha}{2p}\psi^2 + \frac{Z_0}{p^2}(\alpha p - p + \alpha)\psi. \tag{22}$$

The quasineutrality condition $e(n_{i0}-n_{e0}) + n_{d0}q_{d0} = 0$ is realized at equilibrium, i.e. for $\psi = 0$; so Z_0 is the equilibrium charge number. Then, for given values of Z_0, α and f, we have the following relations:

$$\varepsilon = \frac{f-1}{fZ_0}, \tag{23}$$

$$p = \frac{-1+f\sqrt{\alpha m_e/m_i}}{1+f\sqrt{m_e/\alpha m_i}}, \tag{24}$$

and the consistency relation that determines the electron beam energy,

$$W_e = -\frac{2e^2Z_0}{rp}. \tag{25}$$

Z_0 is generally positive, since the grains are charged preferentially by electrons so that $f > 1$. Then, for typical values of f and α, the value of $-1/p$ is greater than 1, ensuring for $\psi < 1$ that the charge relation (19) is well defined.

Stationary nonlinear electrostatic oscillations for untrapped particles are thus described by (9), with the variable grain charge and potential energy being given by (19) and (22). The trapping regime for electrons, ions and dust grains is reached when $\psi \leqslant -1/\alpha$, $\psi \geqslant 1$ and $\chi \leqslant -\beta$ respectively.

Equation (9) can be written as

$$\frac{d^2\psi}{dX^2} = -\frac{dV(\psi)}{d\psi}, \tag{26}$$

with the pseudopotential

$$V(\psi) = -\frac{4}{f\alpha}\sqrt{1+\alpha\psi} - 4\sqrt{1-\psi} - 4\beta\frac{f-1}{fZ_0}\sqrt{1+\chi/\beta} + C. \tag{27}$$

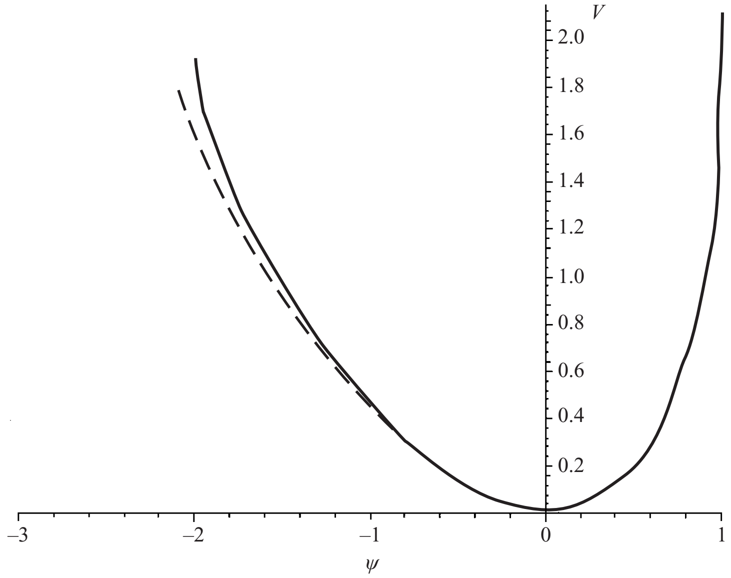

Figure 1. V versus ψ for $Z_0 = 10$, $\beta = 20$, $f = 1.2$ and $\alpha = 0.1$: ——, fixed charge; – – –, with charge variation.

Choosing the condition $V(\psi = 0) = 0$, we obtain for the constant

$$C = 4\left(\frac{1}{f\alpha} + 1 + \frac{f-1}{fZ_0}\beta\right). \tag{28}$$

One can have oscillations only if V is a potential well, or

$$a = \frac{\alpha}{f} + 1 + \frac{f-1}{f}\left(2 + 2p + \frac{Z_0}{\beta} - 2\alpha\right) > 0. \tag{29}$$

This should be compared with the case of fixed grain charge, where the above condition becomes

$$\frac{\alpha}{f} + 1 + \frac{Z_0(f-1)}{\beta f} > 0, \tag{30}$$

which always holds for positive Z_0. Figure 1 compares for $a > 0$ the behaviour of $V(\psi)$ for the cases of fixed and dynamic grain charge. The solutions in the dynamic case are oscillatory modes, and are almost the same as those encountered in the fixed-charge problem.

3. Oscillatory solutions

For small amplitudes (linear theory), i.e. $\psi \gg -1/\alpha$, $\psi \ll 1$ and $\chi \gg -\beta$, the solutions are harmonic modes with wavelength $\sqrt{k}$, where

$$k = 3 - 2\alpha + \frac{3\alpha - 2}{f} + \frac{f-1}{f}\left(2p - 2 + \frac{Z_0}{\beta}\right). \tag{31}$$

The dust charge oscillates around the equilibrium value Z_0.

Figures 2–5 present the results of the numerical integration of the nonlinear problem. The steepening in the profiles of the electric field is the forerunner of wavebreaking due to the approach of the trapping regime, for example trapping of

https://doi.org/10.1017/S0022377801001593 Published online by Cambridge University Press

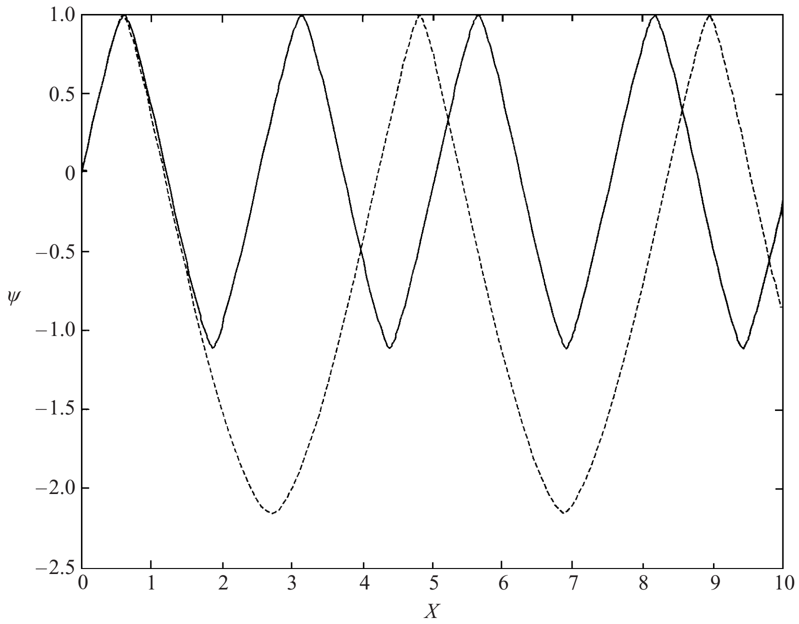

Figure 2. ψ versus X for $\beta = 20$, $Z_0 = 10$, $f = 1.2$, $n_d = 10^5$ and $E_0 = -2$: ——, $\alpha = 0.9$; – – –, $\alpha = 0.1$.

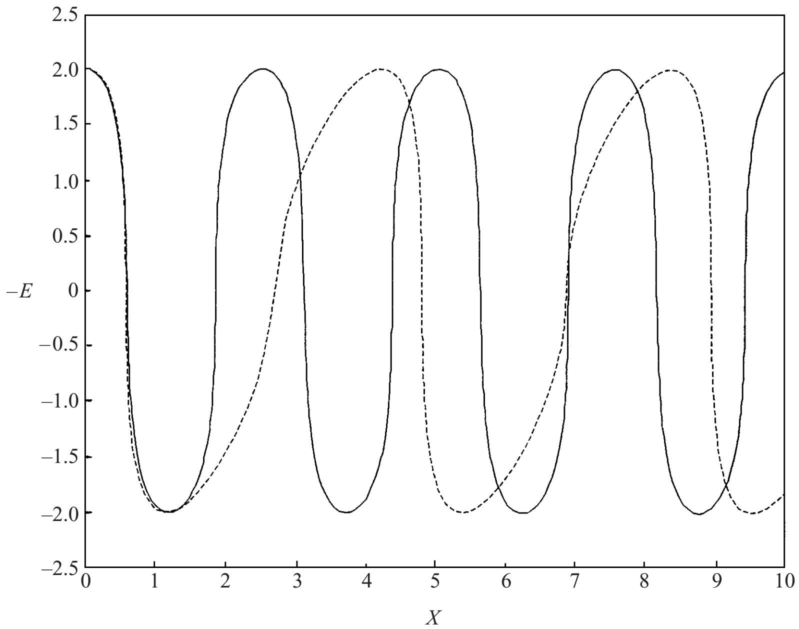

Figure 3. $-E$ ($\equiv d\psi/dX$) versus X for the same parameters as in Fig. 2.

https://doi.org/10.1017/S0022377801001593 Published online by Cambridge University Press

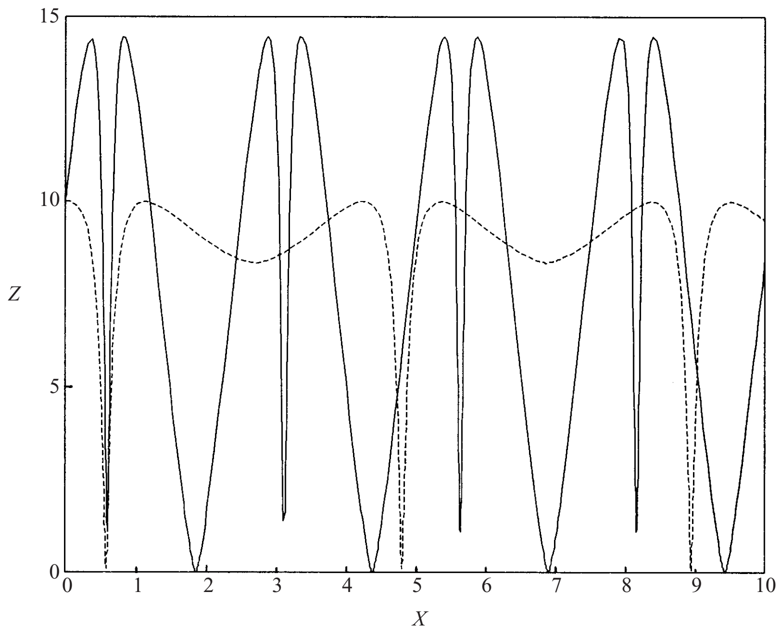

Figure 4. Z versus X for the same parameters as in Fig. 2.

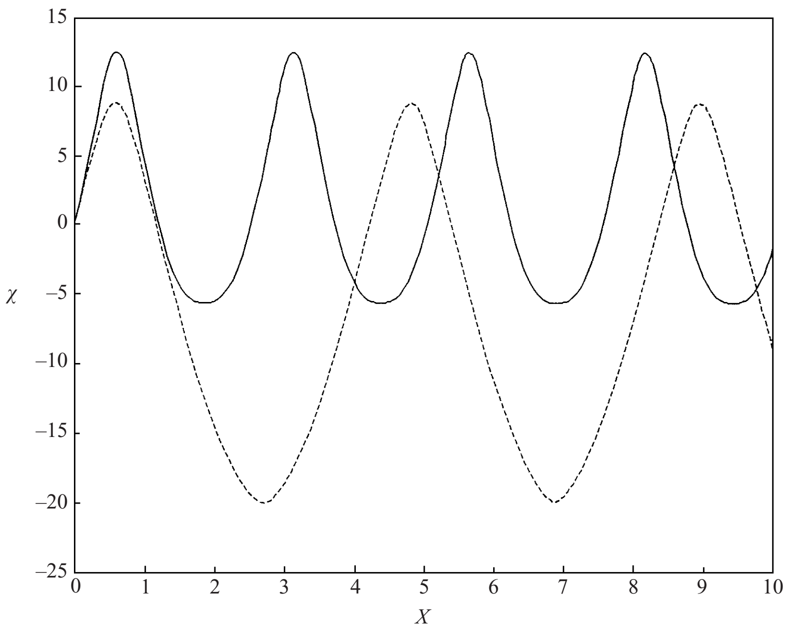

Figure 5. χ versus X for the same parameters as in Fig. 2.

https://doi.org/10.1017/S0022377801001593 Published online by Cambridge University Press

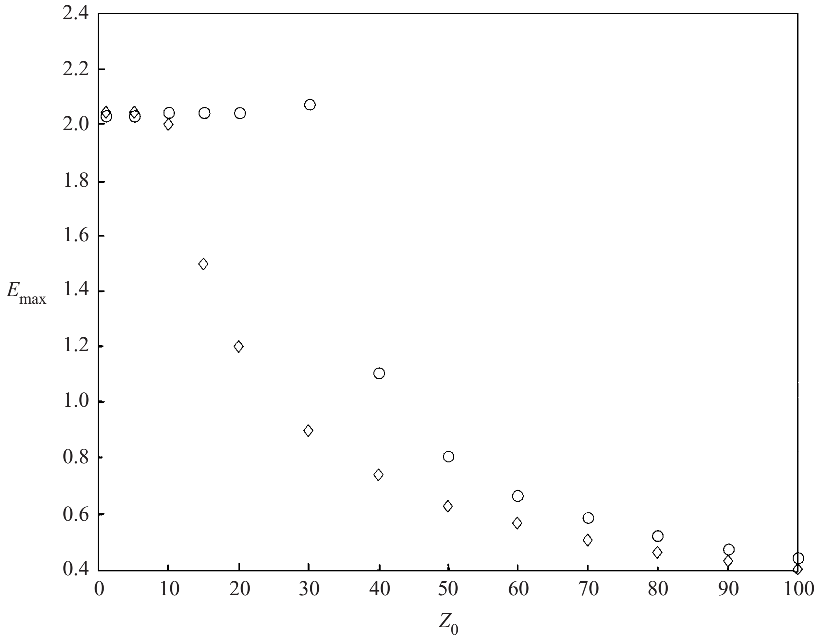

Figure 6. $E_{\max}$ versus Z_0 for $\beta = 20$, $Z_0 = 10$, $f = 1.2$ and $n_d = 10^5$: $\diamond$, $\alpha = 0.1$; $\circ$, $\alpha = 0.9$.

ions and electrons (for the case $\alpha = 0.9$) or trapping of ions and dust grains (for the case $\alpha = 0.1$). Figure 4 shows the nontrivial spatial pattern of the dust charge: as ions and electrons are nearly trapped, i.e. v_e and v_i tend to zero; the charge, as seen from (19), vanishes.

We come now to the influence of the grain charge on the maximum amplitude of the electric field of the modes. This is represented in Fig. 6: as the equilibrium charge increases, the amplitude falls exponentially. This limitation of the amplitude by wavebreaking is due to the trapping of the dust grains: as Z_0 increases, the potential energy χ tends rapidly to $-\beta$. When the trapping of electrons only is the cause of the breaking, the maximum amplitude remains constant until the increasing charge Z_0 allows for the trapping of dust; then the maximum amplitude falls off rapidly (circles in Fig. 6).

4. Soliton solutions

We consider now the case $a < 0$ (Fig. 7). The major result is that a soliton solution for ψ is possible, since (i) $V(0) = 0$, (ii) $V''(0) < 0$, (iii) $V(\psi_0) = 0$ and (vi) $V'(\psi_0) > 0$. Figure 8 shows the pseudopotential for a fixed value of f and increasing values of α (qualitatively the same behaviour is obtained for fixed α and increasing f). The amplitude of the soliton determined by $V(\psi_0) = 0$ increases with increasing f and α (for Z_0 and β fixed). Although the analysis presented here concerns a stationary solution, i.e. in a frame moving with the speed of the waves, we can obtain some information about the speed of the soliton, which increases with f and α because it is related to the depth of the pseudopotential. Figures 9–11 give the simulation result for $f = 3$ and $\alpha = 6$, with the initial conditions $\psi(X = 0) = 0$ and $d\psi/dX(X = 0) = 10^{-11}$. This was obtained by an explicit Runge–Kutta (4, 5)

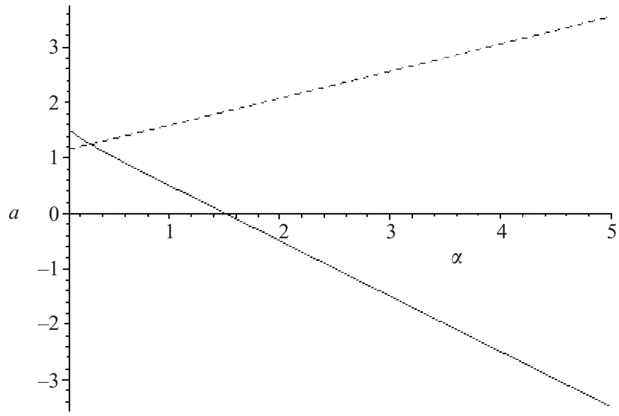

Figure 7. a versus α for $Z_0 = 10$ and $\beta = 20$: ——, $f = 3$; – – –, $f = 1.2$.

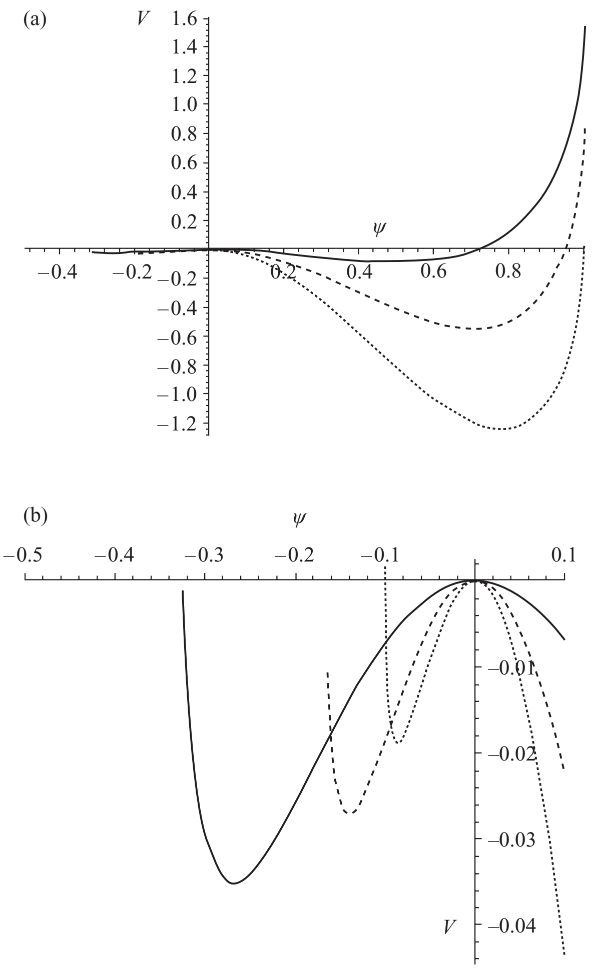

Figure 8. V versus ψ for $Z_0 = 10$, $\beta = 20$ and $f = 3$: ——, $\alpha = 3$; – – –, $\alpha = 6$; · · · · · ·, $\alpha = 10$.

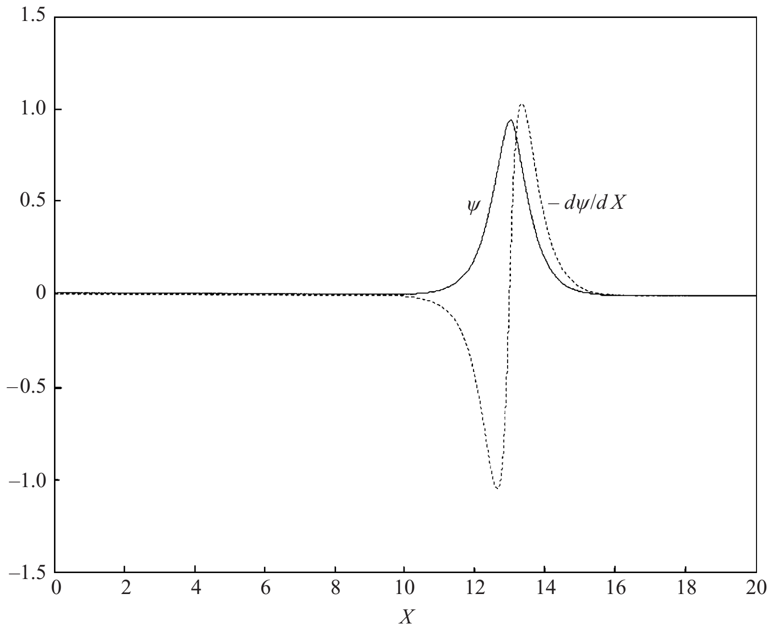

Figure 9. Soliton solution: ——, ψ versus X; – – –, $-d\psi/dX$ versus X. Here $f = 3$, $\alpha = 6$, $\beta = 20$ and $Z_0 = 10$. The initial conditions used in this solution are $\psi(0) = 0$ and $d\psi/dX(0) = 10^{-11}$.

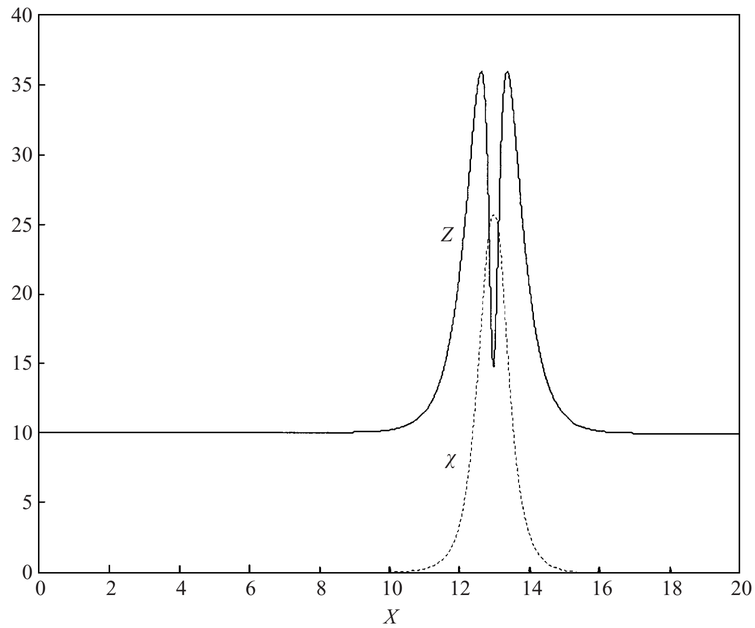

Figure 10. Soliton solution: ——, Z versus X; – – –, χ versus X. The parameters and initial conditions are as in Fig. 9.

https://doi.org/10.1017/S0022377801001593 Published online by Cambridge University Press

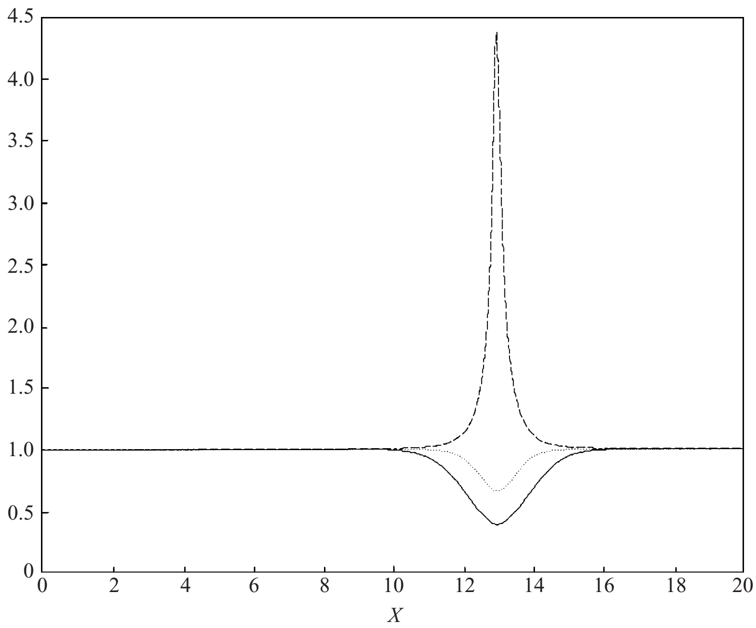

Figure 11. n_i/n_{i0} (– – –), n_e/n_{e0} (——) and n_d/n_{d0} (· · · · · ·) versus X for the case of Fig. 9.

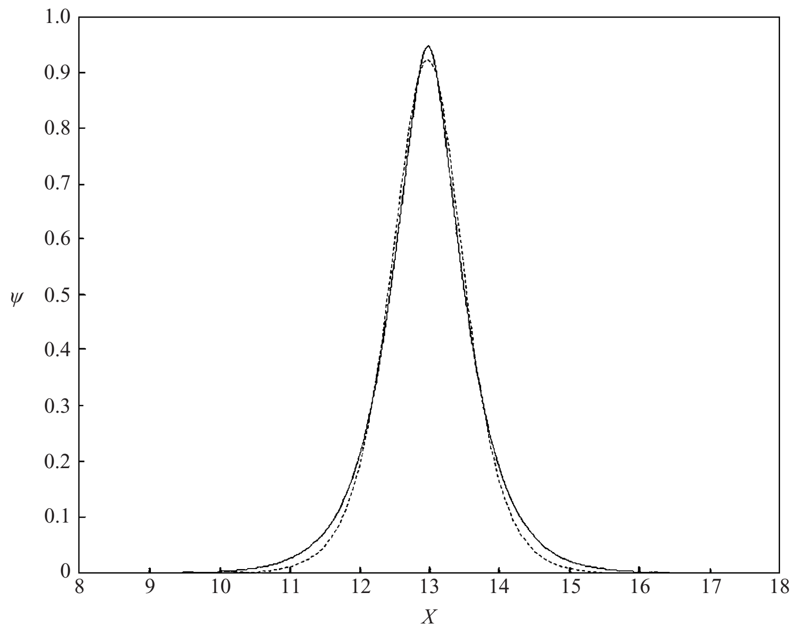

Figure 12. The soliton solution of Fig. 9 (——) and a fitting curve (– – –) based on a sech^2 function (see text for details).

https://doi.org/10.1017/S0022377801001593 Published online by Cambridge University Press

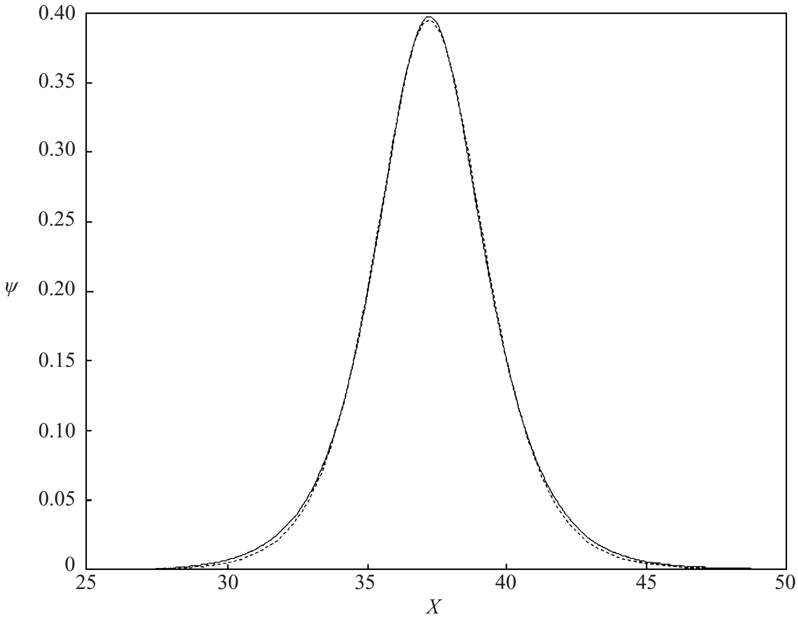

Figure 13. Same as Fig. 12, but for a smaller-amplitude soliton: $\alpha = 2$, $f = 3$, $\beta = 20$ and $Z_0 = 10$.

solver with an absolute tolerance of 10^{-15}. The soliton width at half-amplitude can be calculated numerically by the following integral:

$$\Delta X = 2\int_{\psi_0/2}^{\psi_0} \frac{1}{\sqrt{-V(\psi)}}\, d\psi. \tag{32}$$

We fitted (Fig. 12) the solution of Fig. 9 by a sech^2 profile:

$$\psi(X) = \Psi_0 \,\mathrm{sech}^2[b(X - X_0)] \tag{33}$$

with $\Delta X = 2\ln(1+\sqrt{2})/b$, and found $\Psi_0 = 0.9236$, $b = 1.4630$ and $X_0 = 12.9726$, for which $\Delta X = 0.5455$. For smaller soliton amplitudes (Fig. 13), the solution is better fitted by the sech^2 function, as is well known from the Korteweg–de Vries equation. The parameters for this latter case are $\Psi_0 = 0.3937$, $b = 0.3878$, $X_0 = 37.3011$ and $\Delta X = 1.2048$. The width at half-amplitude found by the fit is the same as that obtained from (32), and, as expected, increases with decreasing soliton amplitude.

We note the 'pit' in the dust-charge profile due to the decrease in ion speed when near the maximum potential for untrapped ions ($\psi = 1$). However, the potential energy of the grains forms a single hump. This solitary electrostatic pulse is formed by a single-hump distribution of ions with a local decrease in the densities of electrons and dust. This is unusual, because the soliton structures known so far are induced by the electron thermal distribution (e.g. ion acoustic solitons: Mamun et al. 1996) and trapped electrons (e.g. electron holes: Lynov et al. 1985). This positive potential soliton with cold untrapped particles is then supported by the space charge of the grains. The fact that it only could be formed for $f \simeq 2$ shows that the electrons are somewhat depleted.

The amplitude of the soliton has maximum value $\psi = 1$ due to the trapping of ions. We note also that for an initial electric field amplitude of the order of 10^{-5} or

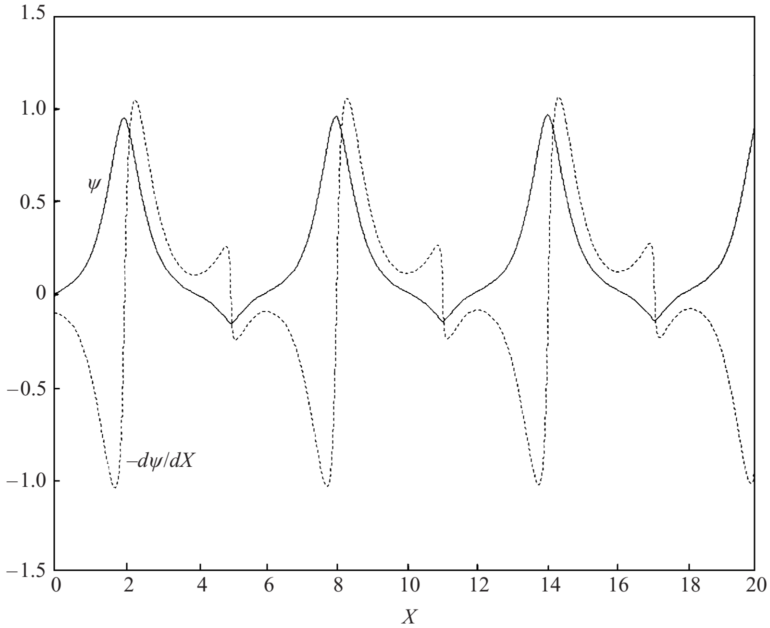

Figure 14. ψ versus X (——) and $-d\psi/dX$ versus X (– – –) for the same parameters as in Fig. 9, but with the initial conditions $\psi(0) = 0$ and $d\psi/dX(0) = 0.1$.

more at $\psi = 0$, we retrieve an oscillatory behaviour (Fig. 14) – but one that is very different from the cases discussed in the previous section. Other oscillatory modes with positive or negative potential can also occur, as is evident from the profiles of Fig. 8.

5. Conclusions

We have considered a cold kinetic model for stationary one-dimensional electrostatic oscillations in a collisionless dusty plasma with variable grain charge. The Bernstein–Greene–Kruskal (BGK) modes for untrapped particles have been identified and their maximum amplitude shown to fall rapidly with increasing dust equilibrium charge owing to the trapping of dust grains. The modes are practically unaltered as compared with the fixed-charge problem. A more important result, which was absent in the fixed-charge problem, is the existence of a soliton solution even in this cold model with untrapped particles. This positive potential pulse is formed by the space charge of dust grains, and depends strongly on the electron density and energy.

A further investigation of these modes requires the introduction of thermal effects and trapped particles. The latter effect can be accounted for through a BGK scheme by first making assumptions on the free-particle part of the distribution function and on $\phi(x)$. One can then calculate the trapped-particle part of the distribution function $f(E)$, which must be positive-definite. Here the variable dust-grain charge may lead to an additional difficulty, because dust grains may interchange their states from trapped to untrapped or vice versa. This will probably introduce more constraints on the yet-unsolved problem of BGK-mode stability.

Acknowledgement

This work was supported in part by the Ministère de l'Enseignement Supérieur et de la Recherche Scientifique Contract D1602/18/99.

References

Barnes, M. S., Keller, H. J., Forster, J. C., O'Neill, J. A. and Coultas, D. K. 1992 *Phys. Rev. Lett.* **68**, 313.

Bernstein, I. B., Greene, J. M. and Kruskal, M. D. 1957 *Phys. Rev.* **108**, 546.

Lynov, J. P., Michelsen, P., Pécseli, H. L., Juul Rasmussen, J. and Sorensen, S. H. 1985 *Physica Scripta* **31**, 596.

Ma, J.-X. and Yu, M. Y. 1994 *Phys. Rev.* **E50**, 50.

Mamun, A. A., Cairns, R. A. and Shukla, P. K. 1996 *Phys. Plasmas* **3**, 702.

Tribèche, M., Hamdi, R. and Zerguini, T. H. 2000 *Phys. Plasmas* **7**, 4013.

Vladimirov, S. V., Ostrikov, K. N., Yu, M. Y. and Stenflo, L. 1998 *Phys. Rev.* **E58**, 8046.

https://doi.org/10.1017/S0022377801001593 Published online by Cambridge University Press